and

$$B\int_0^\infty n^{1-\tau}\exp\left[-\left(k'-\frac{3}{2}\right)\frac{n}{n\xi(k')}\right]dn = QA_1\left(\frac{A_{k+1}}{A_k}\right)^{\sigma\beta}n\xi(k)^{-\sigma\beta} \quad \text{for } p_b \geq p_b{}^c \quad (132)$$

$$B\int_0^\infty n^{k-\tau}\exp\left[-\left(k'-\frac{3}{2}\right)\frac{n}{n\xi(k')}\right]dn = A_k\left(\frac{A_k}{A_{k+1}}\right)^{\sigma\gamma_k}n\xi(k)^{\sigma\gamma_k} \quad k = 2, 3, \ldots \quad (133)$$

Application of the scaling transformation T associated with a positive real number L

$$Tn = Ln, \quad T n\xi = Ln\xi$$
$$Tn_i = Ln_i, \quad i = 1, 2, \ldots, s$$
$$Tl_j = Ll_j, \quad j = 1, 2, \ldots, t \quad (134)$$

to eq 130–133 gives immediately

$$\tau' - s - t - 1 = \sigma\beta$$
$$k + s + t - \tau' = \sigma\gamma_k, \quad k = 2, 3, \ldots \quad (135)$$

and

$$\tau - 2 = \sigma\beta$$
$$k + 1 - \tau = \sigma\gamma_k, \quad k = 2, 3, \ldots \quad (136)$$

with

$$\tau' = \tau + s + t - 1 \quad (137)$$

These relations characterized by the generalized typical size $n\xi(k)$ are a generalization of the scaling law with $k = 2$.[14]

References and Notes

(1) Flory, P. J. *J. Am. Chem. Soc.* **1941**, *63*, 3083, 3091, 3096.
(2) Stockmayer, W. H. *J. Chem. Phys.* **1943**, *11*, 45.
(3) Stockmayer, W. H. *J. Polym. Sci.* **1952**, *9*, 69; **1953**, *11*, 424.
(4) Tang, A.-c.; Kiang, Y.-s. *Sci. Sin. (Engl. Ed.)* **1963**, *12*, 997.
(5) Tang, A.-c. *The Statistical Theory of Polymeric Reactions (Chinese)*; Science Press: Beijing, China, 1981; Chapter 2.
(6) Kiang, Y.-s. *Acta Sci. Nat. (Chinese)* **1962**, *1*, 135.
(7) Flory, P. J. *J. Am. Chem. Soc.* **1947**, *68*, 30.
(8) Gordon, M. *Proc. R. Soc. London, A* **1962**, *268*, 240.
(9) Macosko, C. W.; Miller, D. R. *Macromolecules* **1976**, *9*, 199.
(10) Miller, D. R.; Macosko, C. W. *Macromolecules* **1976**, *9*, 206.
(11) Dusek, K.; Ilavsky, M.; Lunak, S. *J. Polym. Sci., Polym. Symp.* **1975**, *52*, 29.
(12) Peniche-Covas, C. A. L.; Dev, S. B.; Gordon, M.; Judd, M.; Kajiwara, *Faraday Discuss. Chem. Soc.* **1974**, *57*, 165.
(13) de Gennes, P.-G. *Scaling Concepts in Polymer Physics*; Cornell University Press: London, 1979; Chapter 5.
(14) Stauffer, D.; Coniglio, A.; Adam, M. *Adv. Polym. Sci.* **1982**, *44*, 103.

Study of Viscoelastic Relaxation in Amorphous Polypropylene near T_g by Dynamic Light Scattering and Shear Creep

G. Fytas*

Research Center of Crete and Department of Chemistry, University of Crete, Iraklion, Crete, Greece

K. L. Ngai

Naval Research Laboratory, Washington, D.C., 20375-5000.

Received March 13, 1987; Revised Manuscript Received September 8, 1987

ABSTRACT: Polarized photon correlation measurements of completely amorphous polypropylene at temperatures between 268 and 293 K are reported. The time correlation functions of density fluctuation caused by local segmental motion have been represented by the Kohlrausch–Williams–Watts functions. The theory of Wang and Fischer enables us to compute the longitudinal compliance from the time correlation of the density fluctuation. The retardation spectra $L(\log \tau)$ are calculated also formally. Mechanical measurements of the longitudinal or bulk compliances are not available for comparison. However, shear creep measurements have been made by Plazek and Plazek. We find the Kohlrausch exponent of longitudinal compliance from dynamic light scattering agrees rather well with that determined from the local segmental mode contribution to the shear creep. The strong temperature dependence of the effective relaxation time was found to be experimentally identical with that observed for the shift factor of the local segmental mode and the softening transition obtained from shear creep measurements. Thus in the absence of bulk viscoelastic data we may use shear creep measurements to make comparison with dynamic light scattering data. Plazek and Plazek have found the softening dispersion has a different temperature dependence of time scale shift (a_{T_a}) from that of the terminal dispersion or the viscosity (a_{T_η}) in the temperature range of −4.8 to −7.0 °C. The light scattering data have extended this temperature range up to 13 °C in which both these two different shift factors are actually measured and they continue to be different. The combined light scattering and mechanical data are examined in the light of the coupling model of relaxation. The predictions of the model account for the time correlation function observed by light scattering and the time dependence of the creep compliance obtained by mechanical measurements. More importantly the extra prediction of the model can explain the occurrence of two shift factors and relate them quantitatively, in agreement with experimental data.

Introduction

Photon correlation spectroscopy (PCS) is a potential tool in the study of slow thermal density fluctuations in polymer melts near the glass transition temperature (T_g).[1] The density time correlation function measured by PCS has been identified to be related[2] to the time-dependent bulk longitudinal compliance $N(t)$,[3] which otherwise cannot be easily obtained. The first experimental verification of this relation was subsequently carried out in the case of poly(vinyl acetate) (PVAc).[4,5]

The bulk longitudinal stress relaxation modulus $M(t)$ is given by[6] the combination $K + (4/3)G$ of the bulk modulus K and the shear modulus G. It was argued[4,5] that bulk effects predominate in $M(t)$, $K(t) \gg G(t)$ applies, and $M(t)$ is indistinguishable from the bulk modulus. Hence $N(t)$ is also well approximated by the bulk (compressional)

0024-9297/88/2221-0804$01.50/0

compliance $B(t)$. Bulk viscoelastic behavior differs from that in shear. The bulk viscoelastic properties depend only on very local motions or configurational arrangements of the polymer molecules and these are scarcely affected by molecular weight (if sufficiently high), entanglements, or cross-links in moderate numbers. From a molecular standpoint, the local arrangement of polymer molecules responsible for the bulk viscoelastic properties are the same as that which causes volume recovery of an amorphous polymer following a temperature jump near the glass transition temperature T_g studied by Kovacs.[7] It is also closely related to (but not necessarily identical with) the local-mode process observed by dielectric measurements with polymers containing dipoles transverse to the chain backbone.[8] The local segmental motion responsible for transverse dipole relaxation involves conformation transitions and is often called the α-process. We shall adopt these nomenclatures (localized segmental motion or α-relaxation) when referring to the local motions of the polymer molecules that are responsible for its bulk (modulus) compliance and the decay of the time correlation function of the density fluctuation[2] in PCS. In fact for polyvinyl acetate (PVAc) from homodyne PCS measurements, the time correlation of density fluctuation and hence the longitudinal compliance have been determined.[4,5] Mechanical measurements in bulk deformation are rare. Fortunately for a poly(vinyl acetate) of moderately high molecular weight, measurements of the storage and bulk compliance B' and B'' at various temperatures and pressures have been made by McKinney and Belcher.[9] Good agreement between the PCS data and the mechanical bulk compliance data has been demonstrated.[4,5] The bulk loss compliance B'' is zero within experimental error at low and high frequencies and it passes through a maximum in the frequency region of the local segmental mode. Similarly, the retardation spectrum $L_B(\ln \tau)$ obtained from light scattering data or from dynamic compliance data is a broad single peak occurring in a region of retardation times corresponding to that of the local segmental motion.

In most cases other than PVAc, bulk compliance data are not available although shear creep compliance data are. It is desirable to have a procedure to identify the contribution to shear creep compliance from the local segmental mode and locate its time scale and the time dependence of its compliance function (equivalently its retardation spectrum[10]). Only after the characteristics of the local segmental mode have been obtained from the shear creep data can the comparison between light scattering and the mechanical creep data be carried out. The discussions in the following paragraphs will lead us to the procedure for such determination, which will be implemented in a later section.

In addition to the localized segmental motion in a chain, there are other modes of motion of the macromolecular backbone corresponding to the overall rotation and large-scale deformation of the macromolecule. There are various theories of the dynamics of flexible chains that describe these slower and larger scale deformation modes of flexible polymer chains. These include the bead–spring model of Rouse and the local-jump model.[8] We shall refer to these as chain modes in this paper. Both the localized segmental (α) mode and the chain modes contribute to shear viscoelastic properties in the transition from glasslike to rubberlike consistency. In uncross-linked polymers of high molecular weight, the local segmental motion and the chain modes of chain segments between the entanglements contribute to the glass–rubber transition. Described by the shear creep compliance $J(t)$, the glass–rubber transition corresponds to a gradual rise of $J(t)$ with time. In the low molecular weight polymers of narrow distribution this rise occurs in a single stage. While for the high molecular weight polymers after the initial rise of $J(t)$ in the glass–rubber transition, $J(t)$ tends to level off at the plateau compliance J_N^0 to be followed by a final rise from J_N^0 to the steady-state compliance J_e^0 in the terminal zone, attributed to entanglement coupling between polymer chains. The relative contributions to $J(t)$ in the glass–rubber transition region from the α-process and the chain modes are usually not clearly discussed in the literature. There have been attempts to separate those two contributions.[11] The retardation spectrum $L_J(\ln \tau)$ defined formally by the relationship

$$J(t) = J_g + t\eta^{-1} + \int_{-\infty}^{\infty} L_J(\ln \tau)(1 - e^{-t/\tau})\, d \ln \tau \quad (1)$$

where J_g is the glassy compliance, η is the viscosity, and τ is the retardation time offers some help in separating these various contributions.

The $L_J(\ln \tau)$ obtained numerically from $J(t)$ data via eq 1 have common features shared by moderately high molecular weight linear amorphous polymers including atactic polypropylene studied in this work.[12] At the shortest times and above the glassy compliance, there is a time range for which $L_J(\ln \tau) \propto (\ln \tau)^\beta$ where β is close to $^1/_3$. This characteristic first departure from the glassy level has been referred to as Andrade creep.[6,12-16] When a polymer exhibits a rubbery plateau in the compliance, a fairly symmetrical peak is found in $L_J(\ln \tau)$ following the Andrade region just mentioned. This peak has been called the softening peak which indicates the location of the highest population of viscoelastic mechanisms leading to the rubbery compliance J_N^0. The rise from the Andrade region to the softening peak occurs at a time scale approximately where the recoverable shear creep curve has a point of inflection. We have consistently[16] attributed the viscoelastic mechanism contributing to the creep compliance in the Andrade region to the α-process, and in the softening peak to the chain modes. The Andrade region and the softening peak are independent of the molecular weight and its distribution at high molecular weights. In the previous study of the bulk compliance by PCS in PVAc, the polymer samples used in the light scattering and in the mechanical dynamical compliance investigations are different.[4,5] Although this difference is manageable to afford a meaningful comparison, it is desirable to perform light scattering and mechanical measurements of the glass–rubber relaxations on *identical* polymer samples. Such an opportunity of making measurements on identical samples by light scattering and by mechanical means is provided by Donald J. Plazek. He together with Daniel L. Plazek[12] have made shear creep and recovery measurements of completely amorphous polypropylene (PP) between −19 and 71 °C. The resulting compliance curves have covered the viscoelastic behavior above the glassy compliance level from the local segmental mode through the chain modes ["softening" peak in $L_J(\ln \tau)$], the rubbery plateau to the terminal flow region. He has generously supplied us a sample, for light scattering studies, from the same fraction of completely amorphous PP he used for shear creep and viscosity measurements. The number-, weight-, and z-average molecular weights are 6.0×10^4, 1.05×10^5, and 1.44×10^5, respectively. The glass transition temperature was determined to be −14 °C, and the molecular weight per entangled unit was found to be 4650. The experimental window for shear creep measurements extends from $t = 0.45$ s up to 1 day, while that for photon correlation spectroscopy (PCS) extends from $t = 10^{-6}$ s up

to about 10^{-1} s. Thus the two techniques complement each other. We are certainly aware that the PCS measures the longitudinal compliance[2] while shear creep measures shear compliance. The information obtained is not the same. However, as we shall see later in this work, the time dependences as well as the temperature dependences of time-scale shifts for longitudinal and shear compliances contributed by the local segmental motion are nearly the same in amorphous PP. The effective retardation times are somewhat different. Anticipating these results and for reasons to be discussed later, the present light scattering study can be combined with creep compliance measurements to extend the time window within which we can monitor the local segmental motion to the range of 10^{-6} s to 1 day, nearly 11 decades of time. The temperature range of −5 to 13 °C in which the α-relaxation can be probed by PCS in its faster time window overlaps considerably more the temperature range of −2.1 to 70.2 °C of terminal dispersion of shear creep compliance in its slower time window[5] and the temperature range −7 to 70.2 °C of shear viscosity η. Thus PCS data together with shear creep data have significantly enhanced the temperature range in which both the α-process and the terminal process can be observed. From shear creep measurements alone Plazek and Plazek have to make a separate series of viscosity determinations following the attainment of steady-state flow down to −7.0 °C in order to have a limited temperature range, −4.8 to −7.0 °C, which overlaps with the temperature range of −5.45 to −14.4 °C in which the contribution of creep compliance from the local segmental motion appears in the slower time window of creep measurement. Although this overlap is rather limited, they are able to show clearly the values of the shift factor $a_{T\eta}$ obtained from the viscosity is significantly smaller than those obtained from the local segmental and softening dispersion, which precludes time–temperature equivalence or thermorheological simplicity. This conclusion is similar to that reached in other vinyl polymers,[13-15] polystyrene (PS) and poly(vinyl acetate) (PVAc): the local segmental and softening dispersion has a different temperature dependence of time-scale shift ($a_{T\alpha}$) from that of the terminal dispersion (a_{TW}), which is experimentally identical with that of the viscosity $a_{T\eta}$. After the data have been presented, it will be clear that the temperature dependence of the shift factor from PCS data turns out to be the same as that from shear creep. Thus, as far as the shift factor for the local segmental motion $a_{T\alpha}$ is concerned, the temperature range of actual measurements is increased by PCS to the much extended range of −7 to 13 °C. As a result, the PCS data make possible the comparison of actual data of $a_{T\alpha}$ with $a_{T\eta}$ over a considerably more extended temperature range. The new information obtained from this work confirms the large difference between $a_{T\alpha}$ and $a_{T\eta}$ first observed by Plazek and Plazek continues to be the case at higher temperatures that have not been attained before. We shall use the coupling model of relaxation[17] to analyze the PCS and shear creep compliance data, account for the time dependences of the density correlation function and creep compliance, the occurrence of these two shift factors, and the relation between the two temperature dependences. The additional PCS data are in accord with a quantitative relation provided by the coupling model of relaxation.[17] This work demonstrates how a meaningful comparison between dynamic light scattering data and shear viscoelastic data can still be made in the absence of bulk viscoelastic measurements.

Experimental Section

The correlation functions $G(t)$ of the polarized light scattered intensity at different temperatures (268–293 K) were measured for the amorphous atatic polypropyline samples described in the Introduction at a scattering angle of $\theta = 90°$. The light source was an argon ion laser (Spectra Physics 2020) operating at 488.0 nm with a power of 300 mW. The incident beam was polarized vertically with respect to the scattering plane and no polarizer was used for the scattered light. The correlation functions $G(t)$ over 4.3 decades in time were measured with a 28 channel loglin (Malvern K7027) single-clipped correlator in one run. In the present study we used a two-beam heterodyne light beating spectrometer described in ref 18. Heterodyne photon correlation spectroscopic measurements were made because in this manner the desired normalized density time correlation function $g(t)$ associated with the thermal density fluctuations is directly measured, and problems that may arise for a sample that is not 100% dust free are eliminated. In heterodyne detection, $g(t)$ is related to $G(t)$[19] by

$$G(t) = A(1 + b|g(t)|) \tag{2}$$

Where a is the base line measured at long delay times and the amplitude b is considered as a fitting parameter. The base line A is proportional to I_0^2, the intensity of the local oscillator, and $b \sim I_s/I_0$ where I_s is the intensity of the scattered light. The heterodyne condition was experimentally checked by verifying that the contrast b is inversely proportional to the intensity of the local oscillator. Details of the heterodyne technique and comparison with the homodyne technique will be described for amorphous poly(cyclohexyl methacrylate).[20]

Light scattering in amorphous polypropylene comes entirely from density fluctuations. Contribution from anisotropy fluctuations is negligible.

Data Analysis. The net experimental correlation function $[G(t)/A - 1]$ with fixed base line was used to process the data. The Kohlrausch–Williams–Watts (KWW) fractional exponential decay[17,21] function for $g(t)$

$$g(t) = \exp[-(t/\tau^*_\alpha)^\beta] \qquad 0 < \beta \leq 1 \tag{3}$$

such that

$$[G(t)/A - 1] = b \exp[-(t/\tau^*_\alpha)^\beta] \tag{4}$$

fits well the experimental correlation functions, treating b, β, and τ^*_α as adjustable parameters. The normalized correlation functions $g(t)$ measured at a number of temperatures are plotted versus log t in Figure 1. The value of the shape parameter β is equal to 0.36 ± 0.02 and is virtually independent of temperature in the temperature range studied as is the case of PVAc. The nearly constant shape of the correlation functions of Figure 1 suggests that all data can be reduced to the same curve by time–temperature superposition familiar in reduction of viscoelastic data.[6] The reference temperature was chose to be 279.4 K, and all the normalized correlation functions were simply shifted along the time scale by a factor $a_{B\alpha}(T)$.[22] The subscripts $B\alpha$ are used here for the shift factor to remind us that the bulk compliance (B)

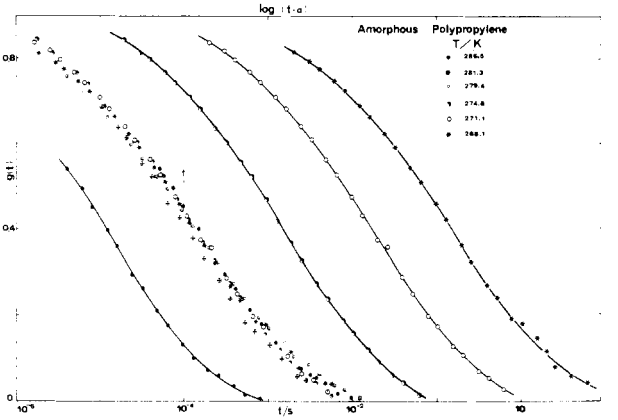

Figure 1. Normalized correlation functions $g(t)$ for amorphous bulk polypropylene at different temperatures plotted versus log t. The reduced curve at 279.4 K was obtained by shifting the experimental correlation functions along the time scale by the factor $a_\alpha(T)$ given via eq 9.

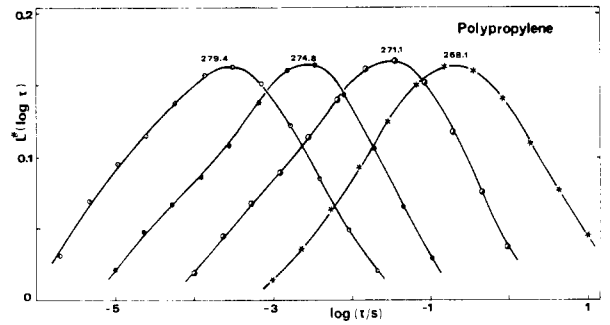

Figure 2. Normalized retardation spectra (L/b) plotted versus log t for polypropylene at four temperatures obtained from the inversion of the correlation functions eq 6.

contributed by local segmental α-relaxation is essentially measured by PCS. As shown in ref 2, 4, and 5, $g(t)$ probed in the PCS experiment is related to bulk compliance $B(t)$ by

$$B(t) = B_\infty + (B_0 - B_\infty)[1 - g(t)] \quad (5)$$

where B_0 and B_∞ are the zero and high-frequency compliances, respectively. If $D(t)$ is written in terms of the retardation function $L(\ln \tau)$ as[4]

$$B(t) = B_\infty + (B_0 - B_\infty)\int_{-\infty}^{\infty} L_B(\ln \tau)(1 - e^{-t/\tau})\, d \ln \tau \quad (6)$$

then

$$g(t) = \int_{-\infty}^{\infty} L_B(\ln \tau) e^{-t/\tau}\, d \ln \tau \quad (7)$$

We have followed an earlier paper[4] in explicitly taking the factor $(B_0 - B_\infty)$ outside the integral in eq 6. An algorithm developed by Provencher[23] is used to calculate $L_B(\ln \tau)$ from eq 7 with $g(t)$ as obtained from measurement. This contrained inverse Laplace transform (ILT) has been modified to yield the $L(\ln \tau)$ of viscoelastic systems.[24] When the correlation functions are well represented by a single KWW decay (eq 3) the numerical technique used to compute the $L(\ln \tau)$ gives experimentally identical result with Provencher's ILT technique.[24] For poly(methyl methacrylate), however, the ILT analysis seems to reveal more clearly the underlying structure of the $g(t)$.[1]

Figure 2 shows the ILT results of the experimental correlation functions for PP at four temperatures above T_g. Actually, we have plotted the ratio $L_B(\ln \tau)/b$. As expected from the nearly constant β and b values (eq 2 and 3), the shape of $L_B(\ln \tau)$ or $L_B(\log \tau)$ is insensitive to temperature variations.

Results and Discussion

If we use $L(\log \tau)$ for the spectrum of retardation time the average $\langle \log \tau \rangle$ is given by the first moment of the $L(\log \tau)$.

$$\langle \log \tau \rangle = \int_0^\infty \log \tau\, L_B(\log \tau)\, d \log \tau \Big/ \int_0^\infty L_B(\log \tau)\, d \log \tau \quad (8)$$

For near symmetric distributions, $\langle \log \tau \rangle$ is close to the logarithm of the average time $\langle \tau \rangle$. The results for $\langle \log \tau \rangle$ are shown in Figure 3. Over the temperature range of −5.1 to 12.3 °C the mean $\langle \log \tau \rangle$ changes by more than 4 orders of magnitude with an unrealistic high Arrhenius activation energy of 85 kcal/mol. We have therefore fitted the Vogel–Fulcher–Tamman–Hesse (VFTH) equation

$$\langle \log \tau \rangle = \langle \log \tau_\infty \rangle + (B/2.303)/(T - T_0) \quad (9)$$

to the experimental $\langle \log \tau \rangle$ values. In the VFTH equation, which is an alternative form of the WLF equation,[15] $\langle \log \tau_\infty \rangle$, B, and T_0 are the characteristic parameters.

To determine these parameters in fairly narrow temperature ranges we adopted the value of −40 °C for the reference temperature T_0 used by Plazek and Plazek for the shear mechanical shift factor of the local segmental

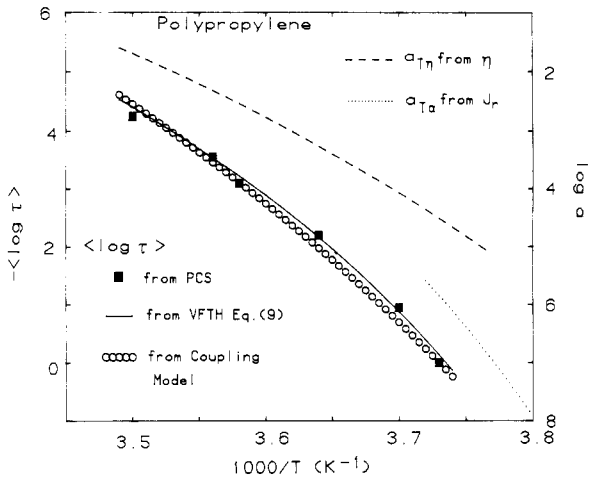

Figure 3. Temperature dependences of the average $\langle \log \tau \rangle$ from photon correlation studies (filled squares) and the time-scale shifts $a_{T\alpha}$ for the local segmental motion (dotted curve) and $a_{T\eta}$ for the viscosity (dashed curve) from shear creep and creep recovery studies (Plazek and Plazek) of amorphous polypropylene. The calculated temperature dependence of $\langle \log \tau \rangle$ obtained from a prediction of the coupling model is shown as the beaded curve. The dotted curve is terminated at −5.4 °C, the highest temperature reached in the measurement of the contribution to the creep compliance from the local segmental mode. The dashed curve is terminated at −7.0 °C, the lowest temperature reached in the viscosity measurement. By inspection, the overlap in the temperature regions of measurements of $a_{T\alpha}$ and $a_{T\eta}$ by creep compliance is limited, but it is considerably enhanced by inclusion of the PCS data.

motion and the softening dispersion.[12] We then obtained from the fit of eq 9 to the experimental values of $\langle \log \tau \rangle$ the values for the other parameters, $\langle \log \tau_\infty \rangle = -12.9$ (τ_∞ in seconds) and $B = 1032$ K. The quality of the fit can be seen by inspection of Figure 3.

The shift factor $a_{T\alpha}$ determined by Plazek and Plazek[12] in the temperature range of −5.4 to −14.4 °C for the local segmental motion and softening dispersion has previously been found to obey also the VFTH equation

$$a_{T\alpha} = A_0 \exp[1027/(T + 40\ °C)] \quad (10)$$

or

$$\log a_{T\alpha} = \log A_0 + 446/(T + 40\ °C) \quad (11)$$

Note that the B parameter from shear compliance is 1027 K from eq 10 which is nearly the same as the value of 1032 K obtained from light scattering. Since the same reference temperature $T_0 = -40$ °C is used in eq 9 and 10, the same values for B mean the longitudinal (bulk) compliance and the shear compliance contributions by the local segmental motion have the same temperature dependence in amorphous PP. This offers in PP an opportunity of combining shear creep and PCS data in the study of the local segmental relaxation to extend considerably the temperature range of measurement and its overlap with the temperature range in which viscosity and terminal dispersion measurements have been made (see discussions in the Introduction).

It would be necessary to characterize more fully the shear compliance contribution from the local segmental motion before we return to discuss the temperature dependences. We shall analyze Plazek and Plazek's shear creep data in the compliance region ($-10 < \log J_R < -8$) where we expect the contribution from the local segmental motion to dominate J. The method of analysis has been discussed in an earlier paper.[16] A KWW form

$$G(t) = G_0 - (G_0 - G_\infty)e^{-(t/\tau^*_G)\beta_G} \quad (12)$$

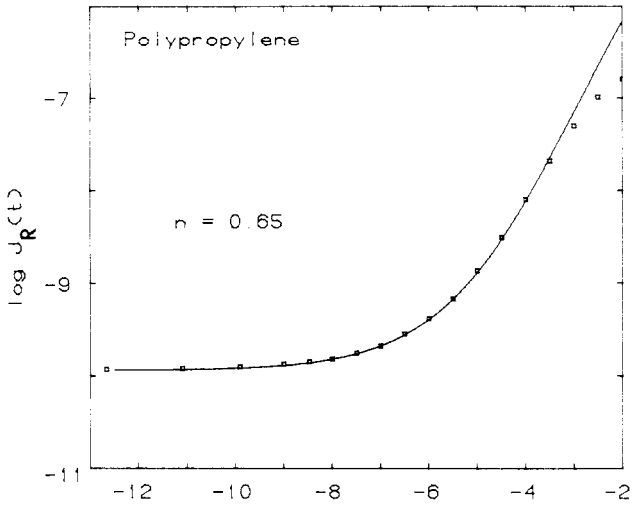

Figure 4. Logarithmic recoverable creep compliance $J_R(t)$ shown as a function of the logarithmic reduced time scale t/a_T in the softening region. Solid curve is the fit to the data for $n_G \equiv 1 - \beta_G = 0.65$ by $J_R(t)$ generated from solutions to eq 13 and 12.

is assumed for the shear modulus G. The family of shear compliance $J(t)$ for different values of β_G is then calculated numerically by deconvoluting the viscoelastic relation

$$\int_0^t J(t)G(t-\tau)\,d\tau = t \tag{13}$$

By comparing the family of $J(t)$'s calculated this way with experimental data (kindly provided to us in numerical form by D. J. Plazek), we can determine the Kohlrausch exponent β_G for shear modulus of PP. At the same time, through this procedure we can determine the effective relaxation time τ^*_G and the effective retardation time τ^*_J at the temperatures measurements were made. In Figure 4 we plot the best fit of $J(t)$ obtained for $\beta_G = 0.35$ to the data reduced to a reference temperature. In the actual practice of fitting the creep compliance data in Figure 4 we have assumed G_0 is small compared with G_∞. Comparison of calculated $J(t)$ with data is made only for those having compliances smaller than the value of about 10^{-8} cm^2/dyn, which is the level at which the data, when plotted as log $J(t)$ versus log t, has an inflection point, and departure from the Andrade region has already occurred. The shift factor for α-relaxation given in eq 11 is then used to find the effective relaxation time τ^*_J at $T = 279.4$ K and other temperatures of PCS investigations. In this manner we can achieve a comparison of τ^*_J with either τ^*_α in eq 3 or, near equivalently, the location of the maximum of $L_B(\ln \tau)$ as shown in Figure 5. At 279.4 K we found $\tau^*_G = 10^{-4.7}$ and $\tau^*_J = 10^{-4.3}$ s from shear creep analysis and $\tau^*_\alpha = 10^{-3.8}$ s for PCS. Hence for the local segmental motion we find its shear retardation time τ^*_J is somewhat shorter than its longitudinal or bulk retardation time τ^*_α, and they have nearly the same temperature dependence for their shift factor. Note that the retardation time of the first peak of the retardation spectrum L_J (see Figure 5 of this work or Figure 7 of ref 4) does not correspond to the retardation time τ^*_J of the local segmental motion. Moreover, without the help of the procedure described, it is not obvious how to locate a characteristic time for the local segmental motion from L_J. Figure 5 shows the normalized dimensionless $L_B/(B_0 - B_\infty)$ spectrum for PP at 279.4 K where B_0 and B_∞ are the limiting isothermal compressibilities. The adiabatic value of B_∞ can be determined by Brillouin scattering and by ultrasonic velocity measurements in the slow relaxation limit. The isothermal B_0 is 2.9×10^{-11} cm^2/dyn at 20 °C[25] and the adiabatic B_∞

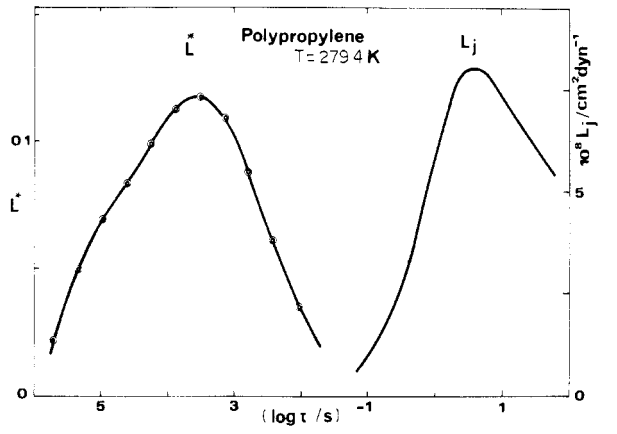

Figure 5. Normalized bulk (L^*) and shear (L_J) retardation spectrum constructed respectively from the present light scattering (circles) and shear creep data of Plazek and Plazek reduced to 279.4 K. Only the first peak of L_J is shown.

value approximately amounts to 1.9×10^{-11} cm^2/dyn.[26] The bulk retardation spectrum is therefore about 3 orders of magnitude smaller than the softening peak (see Figure 5) of the shear retardation spectrum $L_j(\log \tau)$,[12] which is associated with the chain modes (defined in the Introduction). The softening peak of L_j in Figure 5 corresponds to longer range chain modes and should not be confused with the local segmental motion. The fit to the creep compliance $J(t)$ via eq 12 and 13 with the KWW function having $\beta = 0.35$ for PP is entirely consistent with the Andrade creep description by Plazek. It gives rise, for not too large τ/τ^*_G, to a contribution to L_j that is proportional to $(\tau/\tau^*_G)^\beta$ which is $(\tau/\tau^*_G)^{0.35}$ for PP, close to the Andrade creep behavior defined by $L_J(\ln \tau)$ proportional to $\tau^{1/3}$. Incidentally (the rise of L_B or L^* in Figure 2 at short times is also approximately of the form τ^β. This is a direct consequence of eq 3 and 7.

From our analysis of Plazek and Plazek's shear creep data we have found the contribution from the local segmental motion can be described by a $J(t)$ obtained from solving eq 12 and 13. The Kohlrausch–Williams–Watts exponent $\beta_G = 0.35$ is nearly identical with that of density correlation function $g(t)$ having $\beta = 0.36 \pm 0.02$ as obtained from PCS data. In addition, the temperature shift factors for the recoverable shear compliance $J(t)$ and density correlation function $g(t)$ follow nearly the same VFTH equation, (10). It is important to reiterate the complementary nature of the two sets of data. The shear compliance data were taken within the time window of $t = 0.45$ s up to 1 day and the temperature range of −14.4 to −5.4 °C, while the PCS data were collected from 10^{-6} to 10 s in the temperature range of −5 to 20 °C.

In a seminal paper on physical aging Kovacs, Stratton, and Ferry[27] have found already in PVAc that the temperature shift factors for shear and volume (bulk) deformations near T_g ($30 < T < 38$ °C) are identical. They conclude that the molecular motions by which these respective deformations are accomplished are very similar. This is the case again for amorphous PP as borne out by our analysis of PCS data discussed in the present work. It would be interesting to make volume recovery measurements in amorphous PP near T_g, compared with the shear compliance data of Plazek and Plazek in the same temperature range, and check if the shift factors agree or not. The information we deduce from PCS data suggests the shift factor of volume recovery will again be close to that of shear compliance.

Finally, the relaxation of the longitudinal modulus of a largely atatic PP of molecular weight 12 000 has been

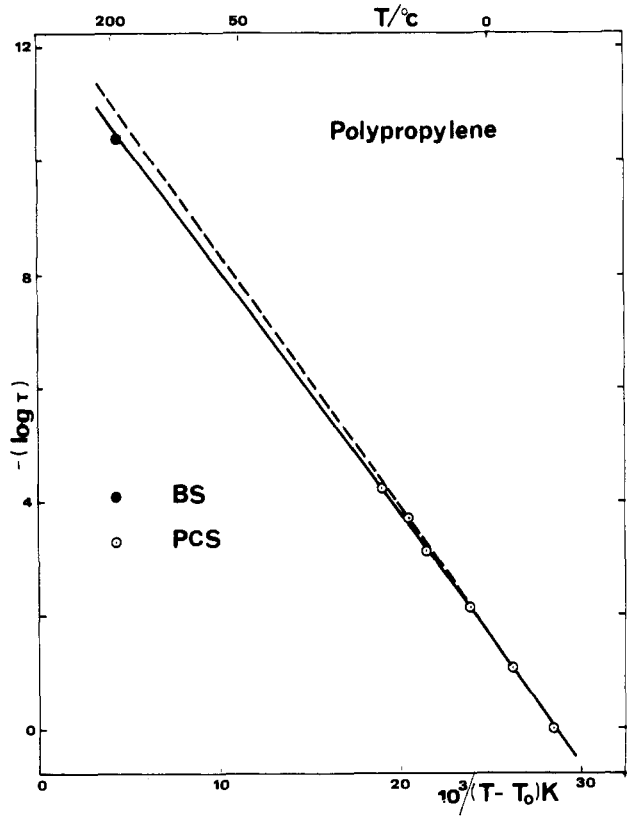

Figure 6. Comparison of the relaxation times for photon correlation spectroscopy (PCS) and Brillouin scattering (BS). Dashed line denotes the extrapolation based only on PCS times. The samples used in PCS and in BS are different.

measured at gegahertz frequencies by using Brillouin spectroscopy (BS).[28] The maximum of the hypersonic absorption occurs at approximately 180 °C and at a frequency f = 4.1 GHz. If the longitudinal modulus is approximated by the modulus of compression and small differences between measurements under isothermal and adiabatic conditions are ignored,[29] then the new fit of eq 9 including the Brillouin relaxation time $1/2\pi f$ yields $(\log \tau_\infty) = -12.4$ and B = 990 K. This situation is illustrated in Figure 6. However, it is worth noting that the structural relaxation time at 180 °C predicted by extrapolation based on the VFTH fit to the photon correlation times (PCS) is faster than the hypersonic measurement. This behavior is similar to that observed for poly(phenylmethylsiloxane)[30] and was interpreted to be due to different β values at low (in PCS measurements) and high (in BS measurements) temperatures. Definite comparison between the results of the two light scattering techniques requires more experimental measurements on the same sample at high temperatures and possibly ultrasonic measurements in the intermediate frequency range.[31] Also since the sample studies in ref 28 by BS may not be completely amorphous as is the case of our present measurements, comparison between the two sets of data may not be justified.

Coupling Model Interpretations. From the investigation of viscoelastic behavior of completely amorphous atatic PP of Plazek and Plazek[12] has emerged the interesting observation of a different temperature dependence near T_g of shear viscosity from that of the recoverable compliance of the local segmental motion. This feature of viscoelastic property has been seen in the vinyl polymers polystyrene[14] and PVAc.[15] One of us together with D. J. Plazek[16] has given explanations of the occurrence of two different shift factors $a_{T\alpha}$ and $a_{T\eta}$ and how they are related to each other quantitatively. The explanations are based on the coupling model of relaxation.[16,17,30] Previously we also have had the occasion to use entirely light scattering techniques to measure the temperature dependences of the self-diffusion of chains and of the local segmental motion in low molecular weight poly(phenylmethylsiloxane) (PPMS).[32] Again we found the two temperature dependences are very different, consistent with Plazek's observations. The predictions of the coupling model were found to be successful, once more, in relating the two shift factors quantitatively.[30]

The availability of the combintion of PCS, shear compliance, and viscosity data of PP will offer a good opportunity to examine the different natures of local segment motion and the viscous deformation. The fact that local segmental motion monitored by the bulk compliance (PCS) and the shear compliance (creep) have the same temperature dependence for their shift factors and the same Kohlrausch exponents, β_G = 0.35 and β = 0.36, justifies a combining the two sets of data in the study of the local segmental motion. This confers a bonus in extending the temperature range in which we can compare $a_{T\alpha}$ that is actually measured with $a_{T\eta}$. These features of the data sets are displayed in Figure 3. Note the temperature range of combined measurements of the local segmental motion by PCS (filled squares) and shear creep (dotted curve) combined now overlaps more extensively with that of the viscous deformation and allows for a stringent test of any model, including the coupling model.

The basis of the coupling model and its predictions has been described previously.[16,17,30] The method of applying the model predictions to the specific problem of relating the two shift factors $a_{T\alpha}$ and $a_{T\eta}$ have been specifically addressed.[16] We refer the reader to these references for details. The notations in ref 16 will be used here again for the purpose of clear connection with our previous work.

In the coupling model approach, the local segmental relaxation has the coupling parameter n_α which can be identified with $(1 - \beta_\alpha)$ where β_α is the Kohlrausch exponent in a KWW representation of its relaxation function. The value of the coupling parameter n_α may depend on the mode of deformation, e.g., bulk or shear. For amorphous PP we have seen from data that whether the local segmental motion is probed either in shear or bulk deformation, the Kohlrausch exponents β_G in eq 12 and β in eq 4 are nearly equal. Hence the values of the coupling parameter n_α for either shear or bulk deformations are almost the same. The situation here is thus rather simple. We do not have to distinguish shear deformation from bulk deformation as far as the coupling parameter of the local segmental motion is concerned. Its value is

$$n_\alpha = 0.64 \tag{14}$$

For the viscous deformation in an entangled polymer melt[33-35] the coupling comes from chain entanglements, and for linear polymer systems we have previously found the coupling constant has the value inside the narrow range of $0.40 \leq n_\eta \leq 0.46$. We shall take the average value of

$$n_\eta = 0.43 \tag{15}$$

which will lead to a molecular weight dependence of $M^{3.5}$ that is consistent with the well-known dependence of $\eta \propto M^{3.4}$. An independent determination of n_η has been obtained also by using the KWW function to fit the terminal dispersion of monodisperse linear polymer melts.

In ref 16 and 30 we introduce the primitive friction coefficient ζ_0 which has its own temperature dependence $\zeta_0(T)$, say a VFTH form due to molecular crowding in the neighborhood of T_g. We have assumed that the primitive

friction factor for the local segmental motion is identical with that for the chain motion.[16,30] As a consequence of the "second relation"[16,17,30] of the coupling model, the relation between the two different shift factors are related by

$$\log (a_{T\alpha}) = [(1 - n_\eta)/(1 - n_\alpha)] \log (a_{T\eta}) \quad (16)$$

This result, derived in ref 16 and 17 and given as eq 29 in ref 16 there, offers a direct comparison with the experimental data of $a_{T\alpha}$ and $a_{T\eta}$ in Figure 3. To carry this out we use the expression

$$\log a_{T\eta} = A'' + 640/(T + 60\ ^\circ\text{C}) \quad (17)$$

given by Plazek and Plazek for the viscosity shift factor and the coupling parameters n_α and n_η given by eq 14 and 15. Substituting these into the right-hand side of eq 16, we arrived at a prediction of the shift factor log $a_{T\alpha}$. To actually compare this prediction with light scattering data, we calculate $\langle \log \tau \rangle$ by the equation

$$\langle \log \tau(T) \rangle = \langle \log \tau(268.1\ \text{K}) \rangle + \log a_{T\alpha}(T) - \log a_{T\alpha}(268.1\ \text{K}) \quad (18)$$

The values of $\langle \log \tau \rangle$ calculated this way are represented by the beaded curve in Figure 3. They are in very good agreement with the PCS data and very nearly coincident with the VFTH fit (solid curve) to the PCS data given earlier by eq 9 Thus it can be concluded that the predicted relation (eq 16) between the two temperature dependences of the shift factors $a_{T\alpha}$ and $a_{T\eta}$ are verified by the additional data of local segmental relaxation in the extended temperature range from −7 to 13 °C made possible by dynamic light scattering.

Without the light scattering data, the temperature range of the shift factor $a_{T\alpha}$ from shear creep measurements alone overlaps that of $a_{T\eta}$ but is limited to a narrower range from −4.8 to −7.0 °C, as depicted in Figure 3. Even within this limited temperature range, Plazek and Plazek were able to conclude the two temperature dependences are different (dashed and dotted curves in Figure 3). The present light scattering data have considerably enhanced the temperature range in which the α-relaxation can be monitored. It provides actual data to temperatures as high as 13 °C to support the continued occurrence of two different shift factors $a_{T\alpha}$ and $a_{T\eta}$.[6,13-15] It has also made the verification of the prediction of the coupling model on this behavior even more convincing. This is a good example of the utility of the light scattering technique to complement mechanical measurements in the investigation of viscoelasticity behavior.

Summary

Through analyses of the photon correlation spectroscopy data and shear creep compliance data of atactic polypropylene, we have found for the local segmental mode the Kohlrausch fractional exponent and the temperature dependence of the shift factor determined from these two different sets of data are in rather good agreement with each other. The effective retardation time τ^*_J of shear creep is about $^1/_2$ an order of magnitude shorter than that of bulk compliance from dynamic light scattering. We have combined dynamic light scattering and shear creep data in characterizing the temperature dependence of the shift factor $a_{T\alpha}$ of the local segmental motion over a very wide experimental window of 10^{-6} s to 1 day. The temperature range over which the local segmental relaxation can be probed has been extended considerably. There is overlap in the temperature ranges of actual measurements of the shift factors $a_{T\alpha}$ and $a_{T\eta}$ of the terminal dispersion or the viscous deformation.

We have also confirmed the interpretation of the physics governing these different relaxation processes as relaxation rate slowing down, the basic starting point of the coupling model.[17] The coupling model has predictions that are in quantitative agreements with the experimental data on the local segmental mode probed either by dynamic light scattering or by creep compliance and separately on the terminal dispersion and the zero-shear viscosity. In particular, it can explain quantitatively the relation between these two different shift factors. It is worthwhile to point out that no other model that we are aware of can address both the local segmental relaxation and the terminal dispersion (or viscous flow) of an entangled polymer system.

Acknowledgment. G. Fytas acknowledges the financial support of the Research Center of Crete. Thanks are due to L. Giebel of the Max Planck Institut fur Polymerforschung in Mainz for his assistance in computation. We thank especially D. J. Plazek for his kindness in supplying us the completely amorphous polypropylene sample and, with D. L. Plazek, tables of his viscoelastic measurements. The work at the Naval Research Laboratory is partially support by ONR Contract N0001487WX24039.

Registry No. PP, 9003-07-0.

References and Notes

(1) See, for example: Patterson, G. D. *Adv. Polym. Sci.* **1983**, *48*, 125. Fytas, G.; Wang, C. H.; Fischer, E. W.; Mehler, K. *J. Polym. Sci., Polym. Phys. Ed.* **1986**, *24*, 1859.
(2) Wang, C. H.; Fischer, E. W. *J. Chem. Phys.* **1985**, *82*, 632.
(3) We use N instead of D to denote the longitudinal compliance in order to avoid the possible confusion with the tensile creep compliance which is also denoted by D in Ferry's text on *Viscoelastic Properties of Polymers*.
(4) Fytas, G.; Wang, C. H.; Meier, G.; Fisher, E. W. *Macromolecules* **1985**, *18*, 1492.
(5) Meier, G.; Hagenah, J.-U.; Wang, C. H.; Fytas, G.; Fischer, E. W. *Polymer* **1987**, *28*, 1640.
(6) Ferry, J. D. *Viscoelastic Properties of Polymers*; Wiley: New York; 1980.
(7) Kovacs, A. J. *Adv. Polym. Sci.* **1964**, *3*, 394.
(8) Stockmayer, W. H. *IEEE Trans. Electr. Insul.* **1985**, *EI-20*, 923.
(9) McKinney, J. E.; Belcher, H. V. *J. Res. Natl. Bur. Stand.* **1963**, *A67*, 43.
(10) Although we shall consider as well as calculate the retardation spectrum of the local segmental motion, we are not interpreting that the dispersion of the local segmental motion is caused by a distribution of retardation times. We regard the retardation spectrum merely as another formal representation of the compliance function of the local segmental motion.
(11) Gray, R. W.; Harrison, G.; Lamb, J. *Proc. R. Soc. London* **1977**, *356*, 77. Cochrane, J.; Harrison, G.; Lamb, J.; Phillips, D. W. *Polymer* **1980**, *21*, 837.
(12) Plazek, D. L.; Plazek, D. J. *Macromolecules* **1983**, *16*, 1469.
(13) Plazek, D. J. *J. Phys. Chem.* **1965**, *69*, 3480; *J. Polym. Sci., Polym. Phys. Ed.* **1968**, *6*, 621.
(14) Plazek, D. J. *Polym. J.* **1980**, *12*, 43.
(15) Plazek, D. J. *J. Polym. Sci., Polym. Phys. Ed.* **1982**, *20*, 729.
(16) Ngai, K. L.; Plazek, D. J. *J. Polym. Sci., Polym. Phys. Ed.* **1986**, *24*, 619 and references therein.
(17) For recent reviews, see: Ngai, K. L.; Rajagopal, A. K.; Rendell, R. W.; Teitler, S. *IEEE Trans. Electr. Insul.* **1986**, *EI-21*, 313; *Ann. N. Y. Acad. Sci.* **1986**, *484*, 150; 321.
(18) Adam, M.; Delsanti, M. *Macromolecules* **1984**, *17*, 782.
(19) Cummins, H. Z.; Pike, E. R. *Photon Correlation and Light Beating Spectroscopy*; Plenum: New York, 1974.
(20) Fytas, G., unpublished results.
(21) Kohlrausch, R. *Pogg. Ann. Phys.* **1847**, *12*, 393. Williams, G.; Watts, D. C. *Trans Faraday Soc.* **1971**, *66*, 80.
(22) The time–temperature superposition of the correlation functions was suggested by Prof. E. W. Fischer.
(23) Provencher, S. W. *Comput. Phys. Commun.* **1982**, *27*, 213.
(24) Hagenah, J.-U.; Meier, G.; Fytas, G.; Fischer, E. W., unpublished results.

(25) Kovacs, A. J.; Stratton, R. A.; Ferry, J. D. *J. Phys. Chem.* **1963**, *67*, 152.
(26) Hellwege, K. H.; Knappe, W.; Lehmann, P. *Kolloid Z. Z. Polym.* **1962**, *183*, 110.
(27) Brandrup, J., Immergut, E. H., Eds. *Polymer Handbook*; Wiley: New York, 1975.
(28) Patterson, G. D. *J. Polym. Sci., Polym. Phys. Ed.* **1977**, *15*, 455.
(29) Drake, P. N.; Dill, J. F.; Montrose, C. J.; Meister, R. *J. Chem. Phys.* **1977**, *67*, 1969.
(30) Ngai, K. L.; Fytas, G. *J. Polym. Sci., Polym. Phys. Ed.* **1986**, *24*, 1683.
(31) Onobajo, A.; Dorfmuller, Th.; Fytas, G. *J. Polym. Sci., Polym. Phys. Ed.*, in press.
(32) Fytas, G.; Dorfmuller, Th.; Chu, B. *J. Polym. Sci., Polym. Phys. Ed.* **1984**, *22*, 1471.
(33) Ngai, K. L.; Rendell, R. W. *Polym. Prep. (Am. Chem. Soc., Div. Polym. Chem.)* **1982**, *23*, 46.
(34) Ngai, K. L.; Plazek, D. J. *J. Polym. Sci., Polym. Phys. Ed.* **1985**, *23*, 2159.
(35) McKenna, G. B.; Ngai, K. L.; Plazek, D. J. *Polymer* **1985**, *26*, 1651.

Equations of State for Polymer Liquids

G. T. Dee* and D. J. Walsh

Central Research & Development Department, E. I. du Pont de Nemours & Co., Inc., Experimental Station, Wilmington, Delaware 19898. *Received May 12, 1987; Revised Manuscript Received August 10, 1987*

ABSTRACT: There are numerous equations of state in the literature which propose to describe polymer liquids. We examine the assumptions on which these various equations are based and compare them using PVT data for a wide range of polymer data. We demonstrate that those theories based on the Lennard-Jones and Devonshire[1] cell model best describe the polymer liquid state. The simple cell model provides a tractable and analytically simple equation of state for the analysis of polymer liquids.

1. Introduction

The most widely used equations of state for polymer liquids are the Flory, Orwoll, and Vrij (FOV)[2] equation, the lattice fluid theory of Sanchez and Lacombe (SL),[3] and the Simha and Somcynsky (SS)[4] hole theory. These theories are based on quite different model assumptions and one might expect that their use in describing polymer liquids would depend strongly on how those assumptions encompass the physics of the polymer liquid state.

To gain some historical perspective into this problem we will first consider the problem of a system of N interacting spherically symmetric molecules. If we divide the system into N cells, then Kirkwood[5] demonstrated that the partition function for this system can be written in the form

$$Z_n = gZ_1 \tag{1.1}$$

where Z_1 is the partition function for a system of N particles which are constrained to remain within their cells (one per cell). For a very dense system, a simple solid, for example, it is trivial to show that the function g is equal to 1. In the opposite extreme of a noninteracting low-density gas, one can show that g takes the value e. This prompted Kirkwood[5] and others to term the function g the "communal entropy" since it reflects changes in the extra entropy in the system as a function of the density. Thus the formalism embodied in eq 1.1 may be a useful description of a system which is close to one of the two extreme cases mentioned above. To proceed with this useful formalism we can further simplify eq 1.1 if we assume that the molecules are confined to the centers of their respective cells. With this approximation Z_n can be written in the following form

$$Z_n = (\lambda^{-3} v_f \exp(-E_0/kT))^n \tag{1.2}$$

where $\lambda = (h^2/mkT)^{1/2}$, m is the mass of a molecule, and E_0 is the potential energy of interaction of a molecule at its origin within its cell with all the other molecules placed at the origins of their respective cells. The function v_f is given by the expression

$$v_f = \int d\vec{a} \exp[-(E(\vec{a}) - E_0)/kT] \tag{1.3}$$

where $E(\vec{a})$ is the interaction energy of a molecule at position $\vec{a}$ within its cell, with all other molecules placed at the origins of their respective cells and the integration is over the cell volume. This construction provides the basis for a class of models which can be termed cell models.[6] The equation of state for this system can then be derived from the following relation

$$p = kT(d(\ln Z_n)/dV)|_T \tag{1.4}$$

In a general case one would obtain contributions to the equation of state from the functions $g(V)$, $v_f(V)$, and $E(V)$. By projecting the problem on to a lattice one simplifies the evaluation of the contributions from $E(V)$ and $v_f(V)$ but one is still left with the formidable problem of evaluating the behavior of g as a function of V.

In practice g is set equal to 1 or e depending on whether or not one is dealing with a system which is dense (a dense subcritical liquid) or a system which is close to a gaslike phase (a low-density supercritical liquid). Clearly one cannot hope that an equation of state derived in this manner will describe a system over a wide range of densities.

To improve on the cell model it was proposed to introduce vacant cells into the system and in this fashion one could describe the extra entropy change in the system as a function of V and T.[6,7] The physical motivation for this idea came from the experimental X-ray evidence.[8] This indicated that density changes in dense liquids occurred with only very small changes in the mean intermolecular separation, indicating that the average coordination number was changing. This type of approach yielded equations of state which described the PVT properties of dense liquids more accurately but at the expense of the inclusion of an ansatz for the function $v_f(V)$.

The proposition that most of the volume change takes place by the presence of holes on a lattice has lead to the development of lattice fluid models[3] of the liquid state. In such models the symmetry of the lattices is used to aid the calculation of the partition function. The lattice size is

0024-9297/88/2221-0811$01.50/0